

Received 19 April 2023, accepted 27 April 2023, date of publication 1 May 2023, date of current version 8 May 2023.

Digital Object Identifier 10.1109/ACCESS.2023.3272038

RESEARCH ARTICLE

State-Transformation-Based Recursive Design Strategy for Leader-Follower Safety Formation Control of Uncertain Multiple Quadrotors

BONG SEOK PARK¹ AND SUNG JIN YOO², (Member, IEEE)

¹Division of Electrical, Electronic, Control Engineering, Institute of IT Convergence Technology, Kongju National University, Cheonan 31080, South Korea

²School of Electrical and Electronics Engineering, Chung-Ang University, Dongjak, Seoul 06974, Republic of Korea

Corresponding author: Sung Jin Yoo (sjyoo@cau.ac.kr)

This work was supported in part by the Research Grant of Kongju National University in 2022, and in part by the National Research Foundation of Korea (NRF) Grant funded by the Korean Government under Grant NRF-2022R1A2C1091658.

ABSTRACT This study is aimed at addressing the adaptive leader–follower safety formation control problem for multiple quadrotors with limited measurement range, unknown disturbances, and thrust saturation. We develop a novel state-transformation-based unified design strategy to solve the underactuation and nonlinear input coupling problems of quadrotors without dividing the outer and inner loop subsystems. First, the state transformation technique is introduced to extract virtual control variables from nonlinear coupled terms combined with the thrust input. Then, a unified formation error is designed to ensure safe formation tracking between the leader and followers with limited measurement range. In the design of a controller, compensating signals using radial basis function neural networks are introduced to compensate for unknown nonlinear terms and develop a modified command-filtered backstepping method. The proposed approach outperforms the existing hierarchical designs and can effectively avoid collisions between quadrotors, even in scenarios with thrust saturation and external disturbances. The Lyapunov stability theory is used to demonstrate that all the errors in the closed-loop system are bounded and can be arbitrarily reduced. Finally, comparative analyses are performed based on simulations to verify the effectiveness of the proposed theoretical approach.

INDEX TERMS Safety formation control, state transformation, multiple quadrotors, underactuated system, limited measurement range.

I. INTRODUCTION

A group of multi-robots can perform complicated tasks more efficiently than a single robot by sharing individual information [1]. In particular, unmanned aerial vehicles are characterized by high mission utilization with low cost and excellent maneuverability [2]. From this point of view, various types of research have been conducted on the formation control of quadrotors because it has the advantage of enabling efficient mission performance due to vertical takeoff and landing. Among these control strategies, the leader-follower approach has been widely used due to its scalability and simplicity (see [3] and the references therein). For successful formation

control, it is necessary to prevent collisions between quadrotors within the measurement range. Therefore, research on formation control must be performed considering the collision avoidance and connectivity preservation problems [4].

A quadrotor is an underactuated system that contains highly nonlinear coupling terms in the position model. To address this problem, control approaches such as proportional-derivative [5], linear-quadratic regulator [6], model predictive control [7], and feedback linearization [8] have been proposed under the assumption that the roll and pitch angles approach zero. However, linearized model-based methods exhibit low efficiencies in translational motion and are vulnerable to external disturbances due to their narrow operating ranges [9]. Nonlinear control methods using the hierarchical strategy have been studied to overcome the

The associate editor coordinating the review of this manuscript and approving it for publication was Qiang Li.

disadvantages of linear control methods. In [10], a time-varying formation tracking method was proposed using the dynamics of the outer loop simplified by a double integrator. Robust control methods, such as H_∞ [11] and the sliding mode control [12], were developed to ensure robustness against disturbances. In [13], an event-triggered formation control method was proposed to improve the battery life. In [14] and [15], neural networks were utilized to handle unknown nonlinear functions. Robust filters were used to address state-dependent disturbances [16]. Reinforcement learning was applied for the model-free formation control of underactuated quadrotors [17]. A distributed consensus control considering a constrained environment was developed for multiple quadrotors [18]. Despite these efforts, the hierarchical design strategy-based methods [10], [11], [12], [13], [14], [15], [16], [17], [18] encounter the following problems: When deriving the desired roll and pitch angles, they are assumed to be equal to the actual angles of the quadrotor. However, this assumption can be restrictive because angular errors occur inevitably during transient responses. Additionally, this framework cannot consider external disturbances in the position model. Therefore, the position-tracking performance of the quadrotor may be degraded. To improve the performance, large torque inputs may be necessary; however, these inputs can reduce the operating time of the quadrotor.

The artificial potential field (APF) method has been widely used due to its real-time operation and concise mathematical description for collision avoidance. In [19], a potential-function-based control method was proposed to avoid intervehicle collisions. A sliding-surface-like variable combining the gradient of the APF [20] and a target avoidance function [21] were developed to avoid collisions between quadrotors and obstacles such as static or dynamic objects. Fuzzy control rules [22] and the rotating potential field [23] were introduced to solve the local minimum problem [24] of the APF. Notably, the design of a controller using the APF method requires a linear combination of independent potential functions for formation tracking and collision avoidance of quadrotors. In this scenario, the time derivatives of the potential functions share the same control input for Lyapunov-based control design. Consequently, it becomes challenging to ensure the stability of the safety formation tracking system when designing a controller.

Motivated by these observations, the objective of this study is to develop a state-transformation-based leader-follower safety formation control design for range-constrained quadrotors. First, we propose a state-transformation-based control method to prevent the position-tracking performance degradation that is typically encountered in hierarchical strategies, which neglect the external disturbances in the position model and transient response of attitude tracking. Using the state transformation technique, the control system is designed recursively without dividing it into two sub-systems as in the hierarchical strategy. Consequently, the position-tracking performance can be improved by considering the attitude angle errors and external disturbances in the

position model. Second, to design a controller that guarantees both formation tracking and collision avoidance, we propose a safe formation control system based on a unified error function. A modified command-filtered backstepping (CFB) and neural networks are used to compensate for unknown nonlinear effects of multiple quadrotors. Finally, the stability of the closed-loop safety formation system is proven using the Lyapunov stability theorem.

The main contributions of this study are twofold: First, compared with the existing hierarchical control strategies [10], [11], [12], [13], [14], [15], [16], [17], [18], we develop a novel state-transformation-based formation control method to relax the assumption that the desired roll and pitch angles are the same as the actual angles of the quadrotor. In this manner, the controller for the position and attitude dynamics can be unified in a recursive design, unlike the existing studies [10], [11], [12], [13], [14], [15], [16], [17], [18] that hierarchically divide the position and attitude dynamics. Consequently, the proposed design approach can consider external disturbances in the position model and transient response of attitude tracking, thereby enhancing the formation tracking performance with low torque inputs and resulting in increased operation time for practical application. Second, a unified error-based design for the safety formation tracking of range-constrained multiple quadrotors is presented to overcome the problem of sharing the same input of the APF methods [19], [20], [21], [22], [23]. Using the unified error, an adaptive formation controller is designed to ensure formation safety, including collision avoidance between the leader and followers within the limited measurement range. Furthermore, the modified CFB approach is used to compensate for unknown nonlinear effects of multiple quadrotors by using neural-network-based compensating signals.

The remaining paper is organized as follows. Section II describes the model and the control objectives. Section III presents the novel state-transformation-based unified design for leader-follower safety formation control. Section IV presents the simulation results to verify the performance of the proposed method. Section V presents the concluding remarks.

II. PRELIMINARIES AND PROBLEM FORMULATION

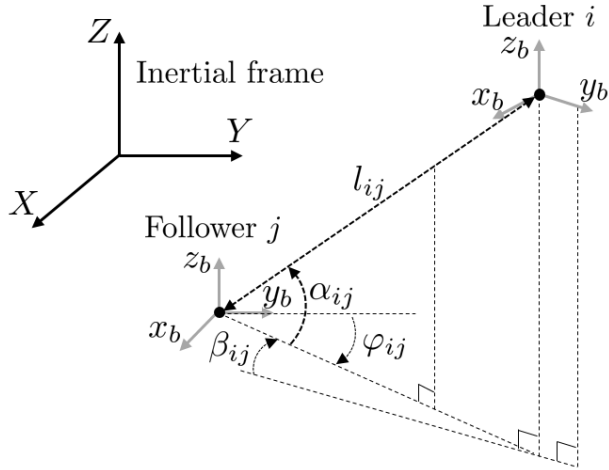
A. QUADROTOR MODEL

The rigid-body model of the j th quadrotor is described as follows [25]:

$$m_j \ddot{p}_j = R_j(q_j)u(F_j) + d_j - m_j G_j \quad (1)$$

$$J_j \ddot{q}_j = C_j(\dot{q}_j) + \tau_j + \tau_{d,j} \quad (2)$$

where $p_j = [x_j, y_j, z_j]^\top$ is the position vector of the center of the mass in the inertial frame, $q_j = [\phi_j, \theta_j, \psi_j]^\top$ is the attitude angle vector describing the orientation of the body-fixed frame, m_j is the total mass of the quadrotor, $G_j = [0, 0, g]^\top$ is the gravitational acceleration vector, d_j and $\tau_{d,j}$ denote the disturbance vectors including unstructured uncertainty and


FIGURE 1. Leader-follower configuration.

wind, F_j is the total thrust force exerted by the four rotors, and $\tau_j = [\tau_{1,j}, \tau_{2,j}, \tau_{3,j}]^T$ is the torque vector in the body-fixed frame. $u(F_j)$ is the output of the saturation function, which is described by

$$u(F_j) = \begin{cases} F_{m,j}, & F_j < F_{m,j} \\ F_j, & F_{m,j} \leq F_j \\ F_{M,j}, & F_j > F_{M,j} \end{cases} \quad (3)$$

where $F_{m,j}$ and $F_{M,j}$ are the known lower and upper bounds of F_j , respectively. The vectors R_j and C_j , and matrix J_j are defined as

$$R_j(q_j)^* = \begin{bmatrix} \sin \psi_j \sin \phi_j + \cos \psi_j \sin \theta_j \cos \phi_j \\ \sin \psi_j \sin \theta_j \cos \phi_j - \cos \psi_j \sin \phi_j \\ \cos \theta_j \cos \phi_j \end{bmatrix}$$

$$J_j^* = \begin{bmatrix} J_{x,j} & 0 & 0 \\ 0 & J_{y,j} & 0 \\ 0 & 0 & J_{z,j} \end{bmatrix}, \quad C_j(\dot{q}_j) = \begin{bmatrix} (J_{x,j} - J_{z,j})\dot{\theta}_j\dot{\psi}_j \\ (J_{z,j} - J_{x,j})\dot{\phi}_j\dot{\psi}_j \\ (J_{x,j} - J_{y,j})\dot{\phi}_j\dot{\theta}_j \end{bmatrix}$$

where $J_{x,j}$, $J_{y,j}$, and $J_{z,j}$ represent the inertia with respect to the body-fixed frame. In these expressions, m_j is assumed to be known, but C_j , J_j , d_j , and $\tau_{d,j}$ are unknown.

Assumption 1: The disturbance vectors d_j and $\tau_{d,j}$ are bounded such that $\|d_j\| \leq \bar{d}_j$ and $\|\tau_{d,j}\| \leq \bar{\tau}_{d,j}$ where \bar{d}_j and $\bar{\tau}_{d,j}$ are unknown constants.

Remark 1: The constraint that the total thrust force F_j of quadrotors must be positive is represented using the saturation function $u(F_j)$ in (1). The values of $F_{m,j}$ and $F_{M,j}$ are selected as $0 < F_{m,j} < F_{M,j}$ when $F_j > 0$.

B. LEADER-FOLLOWER MODEL

The leader-follower model, shown in Fig. 1, is used to design formation controllers for multiple quadrotors. The relative distance l_{ij} , angles of incidence α_{ij} and bearing β_{ij} can be

expressed using the coordinates of the quadrotors as follows:

$$l_{ij} = \sqrt{(x_i - x_j)^2 + (y_i - y_j)^2 + (z_i - z_j)^2}$$

$$\alpha_{ij} = \arctan \left(\frac{z_i - z_j}{\sqrt{(x_i - x_j)^2 + (y_i - y_j)^2}} \right)$$

$$\beta_{ij} = \psi_i - \arctan \left(\frac{y_i - y_j}{x_i - x_j} \right) \quad (4)$$

where subscript i denotes the leader of follower j . The relative distance l_{ij} and angle of incidence α_{ij} can be measured by follower j . The bearing angle β_{ij} can be obtained indirectly from the angle φ_{ij} measured by follower j , i.e., $\beta_{ij} = \varphi_{ij} + \psi_i - \psi_j$. From Fig. 1, the following equations are obtained:

$$x_i - x_j = l_{ij} \cos \alpha_{ij} \cos(\psi_i - \beta_{ij})$$

$$y_i - y_j = l_{ij} \cos \alpha_{ij} \sin(\psi_i - \beta_{ij})$$

$$z_i - z_j = l_{ij} \sin \alpha_{ij}. \quad (5)$$

From (5), the time derivative of (4) is derived as

$$\dot{l}_{ij} = \sin \alpha_{ij}(\dot{z}_i - \dot{z}_j) + \cos \alpha_{ij} \cos(\psi_i - \beta_{ij})(\dot{x}_i - \dot{x}_j) + \cos \alpha_{ij} \sin(\psi_i - \beta_{ij})(\dot{y}_i - \dot{y}_j)$$

$$\dot{\alpha}_{ij} = \frac{\cos \alpha_{ij}}{l_{ij}}(\dot{z}_i - \dot{z}_j) - \frac{\sin \alpha_{ij}}{l_{ij}} \cos(\psi_i - \beta_{ij})(\dot{x}_i - \dot{x}_j) - \frac{\sin \alpha_{ij}}{l_{ij}} \sin(\psi_i - \beta_{ij})(\dot{y}_i - \dot{y}_j)$$

$$\dot{\beta}_{ij} = \dot{\psi}_i + \frac{1}{l_{ij} \cos \alpha_{ij}} \sin(\psi_i - \beta_{ij})(\dot{x}_i - \dot{x}_j) - \frac{1}{l_{ij} \cos \alpha_{ij}} \cos(\psi_i - \beta_{ij})(\dot{y}_i - \dot{y}_j). \quad (6)$$

C. RADIAL BASIS FUNCTION NEURAL NETWORK

According to the universal approximation theory [26], an unknown nonlinear function $f_{n,j}$ can be approximated by the radial basis function neural network (RBFNN) [27] as follows:

$$f_{n,j} = W_{n,j}^T \Phi_{n,j}(\chi_{n,j}) + \varepsilon_{n,j} \quad (7)$$

where $W_{n,j}$ is the optimal weight of the RBFNN, $\varepsilon_{n,j}$ is the reconstruction error, and $\Phi_{n,j} = [\Phi_{n,1,j}, \dots, \Phi_{n,N_j,j}]^T$ is the Gaussian function defined by $\Phi_{n,h,j} = \exp(-(\chi_{n,j} - c_{n,h,j})^T(\chi_{n,j} - c_{n,h,j}) / (2\zeta_{n,h,j}^2))$ for $h = 1, \dots, N_j$; $\chi_{n,j}$ is the input of the RBFNN, N_j is the number of hidden layer nodes, and $c_{n,h,j}$ and $\zeta_{n,h,j}$ denote the center and width of the Gaussian function, respectively. Notably, the Gaussian function $\Phi_{n,j}$ is bounded such that $\|\Phi_{n,j}\| \leq \sqrt{N_j}$.

Property 1: The optimal weight $W_{n,j}$ and reconstruction error $\varepsilon_{n,j}$ are bounded such that $\|W_{n,j}\|_F \leq \bar{W}_{n,j}$ and $\|\varepsilon_{n,j}\| \leq \bar{\varepsilon}_{n,j}$, respectively, where $\bar{W}_{n,j}$ and $\bar{\varepsilon}_{n,j}$ are positive constants and $\|\cdot\|_F$ denotes the Frobenius norm.

D. CONTROL OBJECTIVES

The main objective of this study is to design the control inputs F_j and τ_j for maintaining the desired safety formation of multiple quadrotors under range constraints. To achieve this objective, the following safety formation conditions must be satisfied:

- 1) $r_{a,j} < l_{ij}(t) < r_{c,j}, \forall t \geq 0$;
- 2) $\lim_{t \rightarrow \infty} |l_{d,ij} - l_{ij}| \leq \mu_0, \lim_{t \rightarrow \infty} |\alpha_{d,ij} - \alpha_{ij}| \leq \mu_1,$
and $\lim_{t \rightarrow \infty} |\beta_{d,ij} - \beta_{ij}| \leq \mu_1$;

where μ_0 and μ_1 are arbitrary small constants, $r_{a,j}$ is the minimum avoidance range, $r_{c,j}$ is the maximum measurement range, and $l_{d,ij}, \alpha_{d,ij},$ and $\beta_{d,ij}$ denote the desired distance and angles of incidence and bearing, respectively.

Assumption 2: The desired distance $l_{d,ij}$ and angles of incidence $\alpha_{d,ij}$ and bearing $\beta_{d,ij}$ are constants and bounded such that $l_{d,ij} \in (r_{a,j}, r_{c,j} - r_{a,j}), \alpha_{d,ij} \in (-\pi/2, \pi/2),$ and $\beta_{d,ij} \in [-\pi/2, \pi/2]$. Additionally, the initial distance $l_{ij}(0)$ and the height z_i of the leader robot are given to satisfy $l_{ij}(0) \in (r_{a,j}, r_{c,j})$ and $z_i(t) > l_{d,ij} |\sin \beta_{d,ij}| + r_{a,j}, \forall t \geq 0,$ respectively.

III. MAIN RESULTS

In this section, a state-transformation-based unified control design approach is developed to achieve the formation control objectives without separating the outer and inner loop subsystems. A novel state transformation technique is introduced to solve the underactuation and nonlinear input coupling problems. A unified formation error is derived to ensure safe formation tracking. Finally, the formation controller is designed using the modified CFB.

A. STATE TRANSFORMATION

The position model in (1) has three outputs (x_j, y_j, z_j) and one control input F_j . Moreover, the control input is complexly coupled with trigonometric functions. To address these problems, the state variables ϕ_j and θ_j are transformed as follows:

$$\begin{aligned} \cos \phi_j &= \frac{1}{\sqrt{1 + \bar{\phi}_j^2}}, & \sin \phi_j &= \frac{\bar{\phi}_j}{\sqrt{1 + \bar{\phi}_j^2}} \\ \cos \theta_j &= \frac{1}{\sqrt{1 + \bar{\theta}_j^2}}, & \sin \theta_j &= \frac{\bar{\theta}_j}{\sqrt{1 + \bar{\theta}_j^2}} \end{aligned} \quad (8)$$

where $\bar{\phi}_j$ and $\bar{\theta}_j$ are the transformed state variables defined as $\bar{\phi}_j = \tan \phi_j$ and $\bar{\theta}_j = \tan \theta_j$, respectively.

Substituting (8) into (1) yields

$$\ddot{p}_j = \bar{R}_j(\bar{q}_j) \frac{u(F_j)}{m_j \sqrt{1 + \bar{\phi}_j^2} \sqrt{1 + \bar{\theta}_j^2}} + \frac{d_j}{m_j} - G_j \quad (9)$$

where

$$\begin{aligned} \bar{R}_j(\bar{q}_j) &= \begin{bmatrix} \bar{\phi}_j \sqrt{1 + \bar{\theta}_j^2} \sin \psi_j + \bar{\theta}_j \cos \psi_j \\ \bar{\theta}_j \sin \psi_j - \bar{\phi}_j \sqrt{1 + \bar{\theta}_j^2} \cos \psi_j \\ 1 \end{bmatrix} \\ \bar{q}_j &= [\bar{\phi}_j, \bar{\theta}_j, \psi_j]^T. \end{aligned}$$

Remark 2: The position model of the quadrotor is an underactuated system with one control input F_j and three outputs: $x_j, y_j,$ and z_j . Additionally, the position model combines state variables ϕ_j and θ_j with trigonometrical functions (see $R_j(q_j)u(F_j)$ given in (1)), which makes it challenging to design a recursive control system that unifies the position and attitude dynamics. To address this problem, most of the existing studies [10], [11], [12], [13], [14], [15], [16], [17], [18] have used a hierarchical design strategy. This strategy is aimed at deriving the desired roll $\phi_{d,j}$ and pitch $\theta_{d,j}$ angles under the assumption that $\phi_j = \phi_{d,j}$ and $\theta_j = \theta_{d,j}$. However, this assumption fails to account for attitude angle errors and external disturbances in a real environment, resulting in degraded control performance. To overcome this problem, we introduce the state transformation (8) to transform the position model into the form shown in (9), where transformed state variables $\bar{\phi}_j$ and $\bar{\theta}_j$ are outside the trigonometric functions (see $\bar{R}_j(\bar{q}_j)$ in (9)). This configuration allows the transformed state variables to be used as virtual controls, enabling the design of a recursive control system that considers the attitude errors and external disturbances in the position model.

B. FORMATION CONTROLLER DESIGN

Define the unified formation errors for leader-follower formation tracking with collision avoidance as

$$\begin{aligned} e_{1,j} &= \begin{bmatrix} e_{11,j} \\ e_{12,j} \\ e_{13,j} \end{bmatrix} = \begin{bmatrix} \ln \left(\frac{h_{ij} + \delta_{ij}}{h_{ij}(1 - \delta_{ij})} \right) \\ \alpha_{d,ij} - \alpha_{ij} \\ \beta_{d,ij} - \beta_{ij} \end{bmatrix} \\ e_{2,j} &= \bar{q}_j - [\bar{\eta}_{1,j}^T, \psi_{d,j}]^T \\ e_{3,j} &= \dot{q}_j - \dot{\eta}_{2,j} \end{aligned} \quad (12)$$

where

$$h_{ij} = \frac{r_{c,j} - l_{d,ij}}{l_{d,ij} - r_{a,j}}, \quad \delta_{ij} = \frac{l_{d,ij} - l_{ij}}{l_{d,ij} - r_{a,j}}.$$

$$\Upsilon_{1,j}^{-1} = \begin{bmatrix} \rho_{ij} \cos \alpha_{ij} \cos(\psi_i - \beta_{ij}) & -l_{ij} \sin \alpha_{ij} \cos(\psi_i - \beta_{ij}) & l_{ij} \cos \alpha_{ij} \sin(\psi_i - \beta_{ij}) \\ \rho_{ij} \cos \alpha_{ij} \sin(\psi_i - \beta_{ij}) & -l_{ij} \sin \alpha_{ij} \sin(\psi_i - \beta_{ij}) & -l_{ij} \cos \alpha_{ij} \cos(\psi_i - \beta_{ij}) \\ \rho_{ij} \sin \alpha_{ij} & l_{ij} \cos \alpha_{ij} & 0 \end{bmatrix} \quad (10)$$

$$\Upsilon_{2,j}^{-1} = \begin{bmatrix} \cos^2 \phi_j & 0 & 0 \\ 0 & \cos^2 \theta_j & 0 \\ 0 & 0 & 1 \end{bmatrix}. \quad (11)$$

The vectors $\bar{\eta}_{1,j} = [\bar{\eta}_{11,j}, \bar{\eta}_{12,j}]^\top$ and $\bar{\eta}_{2,j} = [\bar{\eta}_{21,j}, \bar{\eta}_{22,j}, \bar{\eta}_{23,j}]^\top$ are the filtered virtual control laws obtained by the first-order filters such that $\dot{\bar{\eta}}_{n,j} = \gamma_{n,j}(\eta_{n,j} - \bar{\eta}_{n,j})$, where $n = 1, 2$, $\gamma_{n,j}$ are positive constants, and $\eta_{1,j} = [\eta_{11,j}, \eta_{12,j}]^\top$ and $\eta_{2,j} = [\eta_{21,j}, \eta_{22,j}, \eta_{23,j}]^\top$ denote the virtual control vectors. The desired yaw angle $\psi_{d,j}$ is a constant.

Remark 3: If the error $e_{11,j}$ of (12) is bounded at all times, it can be shown that $-h_{ij} < \delta_{ij}(t) < 1$ holds for all $t \geq 0$, given that $h_{ij} > 0$ is ensured from Assumption 2. Using the definition of δ_{ij} , we can deduce that the condition $-h_{ij} < \delta_{ij}(t) < 1$ implies $r_{a,j} < l_{ij}(t) < r_{c,j}$. Thus, the boundedness of $e_{11,j}$ ensures collision avoidance within the limited measurement range for the follower j .

Define the compensated tracking errors for the modified CFB as follows:

$$\begin{aligned} s_{1,j} &= E_j - \xi_{1,j} \\ s_{2,j} &= e_{2,j} - \xi_{2,j} \\ s_{3,j} &= e_{3,j} \end{aligned} \quad (13)$$

where $E_j = [E_{11,j}, E_{12,j}, E_{13,j}]^\top = \dot{e}_{1,j} + \Lambda_{1,j}e_{1,j}$ and $\Lambda_{1,j}$ is a positive-definite matrix. The compensating signals $\xi_{n,j}$ for $n = 1, 2$ are derived from

$$\dot{\xi}_{n,j} = -k_{n,j}\xi_{n,j} + \widehat{W}_{n,j}^\top \Phi_{n,j}(\chi_{n,j}), \quad \xi_{n,j}(0) = 0 \quad (14)$$

where $k_{n,j}$ and $\widehat{W}_{n,j}$ represent the positive design parameters the estimates of optimal weights $W_{n,j}$ of the RBFNNs, respectively.

The update rules of $\widehat{W}_{n,j}$ for $n = 1, 2$ are selected as follows:

$$\dot{\widehat{W}}_{n,j} = \Gamma_{n,j}(\Phi_{n,j}(\chi_{n,j})s_{n,j}^\top - \sigma_{n,j}\widehat{W}_{n,j}) \quad (15)$$

where $\Gamma_{n,j} \in \mathbb{R}^{N_j \times N_j}$ and $\sigma_{n,j} \in \mathbb{R}$ are positive design parameters, $\chi_{1,j} = [l_{ij}, \rho_{ij}, \alpha_{ij}, \beta_{ij}, \bar{q}_j^\top, \bar{p}_j^\top, \dot{p}_j^\top, \eta_{1,j}^\top, \bar{\eta}_{1,j}^\top, \dot{e}_{1,j}^\top, s_{1,j}^\top, \psi_j, \psi_i, \dot{\psi}_i, F_j]^\top$ and $\chi_{2,j} = [q_j^\top, \eta_{2,j}^\top, \bar{\eta}_{2,j}^\top]^\top$.

Remark 4: The conventional CFB is typically used to compensate for the error between the virtual control and its filtered signal in the compensating signal (e.g, $\dot{\xi}_{n,j} = -k_{n,j}\xi_{n,j} + \bar{\eta}_{n,j} - \eta_{n,j}$). To prove closed-loop stability using this method, it is necessary to bound the time derivative of the virtual control, which imposes certain constraints (see Lemmas 1 and 2 in [29] for details). In contrast, the modified CFB uses the outputs of the RBFNNs to define the compensating signals, as shown in (14). Unlike the conventional CFB, the modified CFB does not require the bounds of differentiated virtual controls to analyze closed-loop stability. As a result, the compensating signals using RBFNNs can relax the constraints of the conventional CFB.

The time derivative of (13) along with (2), (6), (9), and (12) is expressed as follows:

$$\begin{aligned} \dot{s}_{1,j} &= \Upsilon_{1,j} \left(\bar{R}(\bar{q}_j) \frac{u(F_j)}{m_j \sqrt{1 + \bar{\phi}_j^2} \sqrt{1 + \bar{\theta}_j^2}} - G_j - \ddot{p}_i + \frac{d_j}{m_j} \right) \\ &\quad + \dot{\Upsilon}_{1,j}(\dot{p}_j - \dot{p}_i) - [0, 0, \ddot{\psi}_i]^\top \\ &\quad + \Lambda_{1,j}\dot{e}_{1,j} - \dot{\xi}_{1,j} \end{aligned} \quad (16)$$

$$\dot{s}_{2,j} = \Upsilon_{2,j}\dot{q}_j - [\bar{\eta}_{1,j}^\top, 0]^\top - \dot{\xi}_{2,j} \quad (17)$$

$$\dot{s}_{3,j} = J_j^{-1}(C_j(\dot{q}_j) + \tau_j + \tau_{d,j}) - \dot{\bar{\eta}}_{2,j} \quad (18)$$

where

$$\begin{aligned} \Upsilon_{1,j} &= \begin{bmatrix} \frac{\cos \alpha_{ij} \cos(\psi_i - \beta_{ij})}{\rho_{ij}} & \frac{\cos \alpha_{ij} \sin(\psi_i - \beta_{ij})}{\rho_{ij}} & \frac{\sin \alpha_{ij}}{\rho_{ij}} \\ -\frac{\sin \alpha_{ij} \cos(\psi_i - \beta_{ij})}{l_{ij}} & -\frac{\sin \alpha_{ij} \sin(\psi_i - \beta_{ij})}{l_{ij}} & \frac{\cos \alpha_{ij}}{l_{ij}} \\ \frac{\sin(\psi_i - \beta_{ij})}{l_{ij} \cos \alpha_{ij}} & -\frac{\cos(\psi_i - \beta_{ij})}{l_{ij} \cos \alpha_{ij}} & 0 \end{bmatrix} \\ \Upsilon_{2,j} &= \begin{bmatrix} \sec^2 \phi_j & 0 & 0 \\ 0 & \sec^2 \theta_j & 0 \\ 0 & 0 & 1 \end{bmatrix} \\ \rho_{ij} &= \frac{(1 - \delta_{ij})(h_{ij} + \delta_{ij})(l_{d,ij} - r_{a,j})^2}{r_{c,j} - r_{a,j}} \end{aligned}$$

The inverse matrices of $\Upsilon_{1,j}$ and $\Upsilon_{2,j}$ exist, as shown at the top of the page.

The following function is defined to facilitate the controller design:

$$\Delta(F_j) = u(F_j) - F_j. \quad (19)$$

From (12), it is obtained that

$$\begin{aligned} \bar{q}_j &= e_{2,j} + [\bar{\eta}_{1,j}^\top, \psi_{d,j}]^\top - [\eta_{1,j}^\top, 0]^\top + [\eta_{1,j}^\top, 0]^\top \\ \bar{q}_j &= e_{3,j} + \bar{\eta}_{2,j} - \eta_{2,j} + \eta_{2,j} \end{aligned} \quad (20)$$

where $\eta_{1,j}$ and $\eta_{2,j}$ are the virtual control laws.

Then, the virtual and actual controls are designed as follows:

$$\eta_{11,j} = \frac{1}{\zeta_{3,j} \sqrt{1 + \bar{\theta}_j^2}} (\zeta_{1,j} \sin \psi_j - \zeta_{2,j} \cos \psi_j) \quad (21)$$

$$\eta_{12,j} = \frac{1}{\zeta_{3,j}} (\zeta_{1,j} \cos \psi_j + \zeta_{2,j} \sin \psi_j) \quad (22)$$

$$\eta_{2,j} = \Upsilon_{2,j}^{-1} (-k_{2,j}e_{2,j} + [\bar{\eta}_{1,j}^\top, 0]^\top - \Upsilon_{3,j}^\top \Upsilon_{1,j} s_{1,j}) \quad (23)$$

$$F_j = m_j \zeta_{3,j} \sqrt{1 + \bar{\phi}_j^2} \sqrt{1 + \bar{\theta}_j^2} \quad (24)$$

$$\tau_j = -k_{3,j}e_{3,j} - \widehat{W}_{3,j}^\top \Phi_{3,j} - \Upsilon_{2,j}^\top s_{2,j} \quad (25)$$

where $k_{n,j}$, $n = 1, 2, 3$ are positive design parameters, $\widehat{W}_{3,j}$ denotes the estimate for the optimal weight $W_{3,j}$ of the RBFNN, and $\zeta_{1,j}$, $\zeta_{2,j}$, and $\zeta_{3,j}$ are given by

$$\begin{bmatrix} \zeta_{1,j} \\ \zeta_{2,j} \\ \zeta_{3,j} \end{bmatrix} = G_j + \ddot{p}_i - \Upsilon_{1,j}^{-1} (k_{1,j}E_j - [0, 0, \ddot{\psi}_i]^\top) - \Upsilon_{3,j}\xi_{2,j} \quad (26)$$

with

$$\Upsilon_{3,j} = \begin{bmatrix} \zeta_{3,j} \sqrt{1 + \bar{\theta}_j^2} \sin \psi_j & \zeta_{3,j} \cos \psi_j & 0 \\ -\zeta_{3,j} \sqrt{1 + \bar{\theta}_j^2} \cos \psi_j & \zeta_{3,j} \sin \psi_j & 0 \\ 0 & 0 & 0 \end{bmatrix}.$$

The update rule of $\widehat{W}_{3,j}$ is selected as follows:

$$\dot{\widehat{W}}_{3,j} = \Gamma_{3,j}(\Phi_{3,j}(\chi_{3,j})s_{3,j}^\top - \sigma_{3,j}\widehat{W}_{3,j}) \quad (27)$$

where $\Gamma_{3,j} \in \mathbb{R}^{N_j \times N_j}$ and $\sigma_{3,j} \in \mathbb{R}$ are positive design parameters, and $\chi_{3,j} = [\dot{q}_j^\top, \dot{\eta}_{2,j}^\top, s_{3,j}^\top, \tau_j^\top]^\top$.

Remark 5: The singularity problem occurs when $\zeta_{3,j} = 0$ in (21) and (22). To address this problem, the design parameter $k_{1,j}$ is chosen as follows:

$$k_{1,j} = \begin{cases} \bar{k}_{1,j} + 1, & \text{if } \bar{k}_{1,j} = \frac{g + \ddot{z}_i}{\rho_{ij}E_{11,j} \sin \alpha_{ij} + l_{ij}E_{12,j} \cos \alpha_{ij}} \\ \bar{k}_{1,j}, & \text{otherwise} \end{cases} \quad (28)$$

where the design parameter $\bar{k}_{1,j}$ is chosen to satisfy $\bar{k}_{1,j} > 1/2$. From the definition of $\zeta_{3,j}$, we have

$$\zeta_{3,j} = g + \ddot{z}_i - k_{1,j}(\rho_{ij}E_{11,j} \sin \alpha_{ij} + l_{ij}E_{12,j} \cos \alpha_{ij}).$$

If $\bar{k}_{1,j} \neq (g + \ddot{z}_i)/(\rho_{ij}E_{11,j} \sin \alpha_{ij} + l_{ij}E_{12,j} \cos \alpha_{ij})$, then $k_{1,j} = \bar{k}_{1,j}$ and thus $\zeta_{3,j} \neq 0$. If $\bar{k}_{1,j} = (g + \ddot{z}_i)/(\rho_{ij}E_{11,j} \sin \alpha_{ij} + l_{ij}E_{12,j} \cos \alpha_{ij})$, then $k_{1,j} = \bar{k}_{1,j} + 1$ and $\zeta_{3,j} = -(\rho_{ij}E_{11,j} \sin \alpha_{ij} + l_{ij}E_{12,j} \cos \alpha_{ij})$. In (28), because the design parameter $\bar{k}_{1,j}$ is chosen as a positive constant, $\bar{k}_{1,j} = (g + \ddot{z}_i)/(\rho_{ij}E_{11,j} \sin \alpha_{ij} + l_{ij}E_{12,j} \cos \alpha_{ij})$ means that $\rho_{ij}E_{11,j} \sin \alpha_{ij} + l_{ij}E_{12,j} \cos \alpha_{ij} \neq 0$ and thus, $\zeta_{3,j} \neq 0$. Therefore, the singularity problem can be eliminated.

Remark 6: Thrust saturation degrades the performance of the closed-loop control system and may cause it to lose stability in a severe environment [30]. For this issue, the compensating signal using the RBFNN is designed to compensate for the difference $\Delta(F_j)$ between the control input and saturated control input. The effect of the difference $\Delta(F_j)$ is included in the unknown function $f_{1,j}$ (see (15)), which is estimated by the RBFNN in the dynamics (14) of the compensating signal $\xi_{1,j}$. Notably, the upper bound of the thrust saturation is determined by manufacturer's specifications and structural limitations of the quadrotor. Therefore, the quadrotors' performance on preserved connectivity and collision avoidance can be maintained within the range allowed by the specifications. If a small upper bound of the thrust saturation exists beyond the range of the specifications, it may not be feasible to achieve formation tracking with collision avoidance. In such a scenario, the desired formation should be appropriately specified to avoid any instability, even with a small upper bound on the thrust saturation.

C. STABILITY ANALYSIS

Substituting (19) and the actual control input F_j in (24) into (16) yields

$$\begin{aligned} \dot{s}_{1,j} = & \Upsilon_{1,j} \left(\bar{R}(\bar{q}_j) \zeta_{3,j} + \bar{R}(\bar{q}_j) \frac{\Delta(F_j)}{m_j \sqrt{1 + \bar{\phi}_j^2} \sqrt{1 + \bar{\theta}_j^2}} \right. \\ & \left. - G_j - \ddot{p}_i + \frac{d_j}{m_j} \right) + \dot{\Upsilon}_{1,j} (\dot{p}_j - \dot{p}_i) \\ & - [0, 0, \dot{\psi}_i]^\top + \Lambda_{1,j} \dot{e}_{1,j} - \dot{\xi}_{1,j}. \end{aligned} \quad (29)$$

Using the virtual control laws (21) and (22), we have

$$\bar{R}(\bar{q}_j) \zeta_{3,j} = \Upsilon_{3,j} [\eta_{1,j}^\top, 0]^\top + [0, 0, \zeta_{3,j}]^\top$$

$$\begin{aligned} & + \Upsilon_{3,j} [\bar{\eta}_{1,j}^\top - \eta_{1,j}^\top, 0]^\top + \Upsilon_{3,j} e_{2,j} \\ = & [\zeta_{1,j}, \zeta_{2,j}, \zeta_{3,j}]^\top + \Upsilon_{3,j} [\bar{\eta}_{1,j}^\top - \eta_{1,j}^\top, 0]^\top \\ & + \Upsilon_{3,j} e_{2,j}. \end{aligned} \quad (30)$$

Substituting (14), (26), and (30) into (29) yields

$$\begin{aligned} \dot{s}_{1,j} = & -k_{1,j} s_{1,j} + \Upsilon_{1,j} \Upsilon_{3,j} s_{2,j} - \widehat{W}_{1,j}^\top \Phi_{1,j} \\ & + f_{1,j} - \frac{\bar{d}_j^2}{2m_j^2 \epsilon_j} \Upsilon_{1,j}^\top \Upsilon_{1,j} s_{1,j} + \Upsilon_{1,j} \frac{d_j}{m_j} \end{aligned} \quad (31)$$

where

$$\begin{aligned} f_{1,j} = & \dot{\Upsilon}_{1,j} (\dot{p}_j - \dot{p}_i) + \Upsilon_{1,j} \Upsilon_{3,j} [\bar{\eta}_{1,j}^\top - \eta_{1,j}^\top, 0]^\top + \Lambda_{1,j} \dot{e}_{1,j} \\ & + \Upsilon_{1,j} \bar{R}(\bar{q}_j) \frac{\Delta(F_j)}{m_j \sqrt{1 + \bar{\phi}_j^2} \sqrt{1 + \bar{\theta}_j^2}} \\ & + \frac{\bar{d}_j^2}{2m_j^2 \epsilon_j} \Upsilon_{1,j}^\top \Upsilon_{1,j} s_{1,j}. \end{aligned}$$

From (17) and (20), we obtain

$$\dot{s}_{2,j} = \Upsilon_{2,j} (e_{3,j} + \bar{\eta}_{2,j} - \eta_{2,j} + \eta_{2,j}) - [\dot{\eta}_{1,j}^\top, 0]^\top - \dot{\xi}_{2,j}.$$

By applying the compensating signal (14) and the virtual control law (23) to the above equation, we obtain

$$\begin{aligned} \dot{s}_{2,j} = & -k_{2,j} s_{2,j} + \Upsilon_{2,j} s_{3,j} - \Upsilon_{3,j}^\top \Upsilon_{1,j} s_{1,j} - \widehat{W}_{2,j}^\top \Phi_{2,j} \\ & + f_{2,j} \end{aligned} \quad (32)$$

where $f_{2,j} = \Upsilon_{2,j} (\bar{\eta}_{2,j} - \eta_{2,j})$.

Substituting the actual control input (25) into (18) yields

$$\begin{aligned} J_j \dot{s}_{3,j} = & -k_{3,j} s_{3,j} - \widehat{W}_{3,j}^\top \Phi_{3,j} - \Upsilon_{2,j}^\top s_{2,j} \\ & + \tau_{d,j} + f_{3,j} - \frac{\bar{\tau}_{d,j}^2}{2\epsilon_j} s_{3,j} \end{aligned} \quad (33)$$

where

$$f_{3,j} = C_j(\dot{q}_j) - J_j \dot{\eta}_{2,j} + \frac{\bar{\tau}_{d,j}^2}{2\epsilon_j} s_{3,j}.$$

The following theorem provides the main result of this paper.

Theorem 1: If the control inputs given in (25) with the update rules provided in (15) and (27) are applied to the leader-follower model (6) satisfying Assumptions 1–2, then there exist design parameters for achieving the control objectives for any initial conditions. Furthermore, the proposed approach ensures that the formation errors can be made arbitrarily small, thereby guaranteeing the desired safety formation of multiple quadrotors.

Proof: Consider the following Lyapunov function candidate:

$$V = \frac{1}{2} \left(\sum_{n=1}^2 s_{n,j}^\top s_{n,j} + s_{3,j}^\top J_j s_{3,j} + \sum_{n=1}^3 \text{tr}(\tilde{W}_{n,j}^\top \Gamma_{n,j}^{-1} \tilde{W}_{n,j}) \right)$$

where $\tilde{W}_{n,j} = W_{n,j} - \widehat{W}_{n,j}$ and $\text{tr}(\cdot)$ denotes a trace of matrix.

The time derivative of V along with (31), (32), and (33) is expressed as

$$\begin{aligned} \dot{V} = & s_{1,j}^\top \left(-k_{1,j}s_{1,j} + \Upsilon_{1,j}\Upsilon_{3,j}s_{2,j} + f_{1,j} - \widehat{W}_{1,j}^\top \Phi_{1,j} \right. \\ & \left. - \frac{\bar{d}_j^2}{2m_j^2\epsilon_j} \Upsilon_{1,j}^\top \Upsilon_{1,j}s_{1,j} + \Upsilon_{1,j} \frac{d_j}{m_j} \right) \\ & + s_{2,j}^\top (-k_{2,j}s_{2,j} + \Upsilon_{2,j}s_{3,j} - \Upsilon_{3,j}^\top \Upsilon_{1,j}s_{1,j} \\ & \quad + f_{2,j} - \widehat{W}_{2,j}^\top \Phi_{2,j}) \\ & + s_{3,j}^\top \left(-k_{3,j}s_{3,j} + f_{3,j} - \widehat{W}_{3,j}^\top \Phi_{3,j} - \Upsilon_{2,j}^\top s_{2,j} \right. \\ & \quad \left. + \tau_{d,j} - \frac{\bar{\tau}_{d,j}^2}{2\epsilon_j} s_{3,j} \right) \\ & - \sum_{n=1}^3 \text{tr}(\tilde{W}_{n,j}^\top \Gamma_{n,j}^{-1} \dot{\tilde{W}}_{n,j}). \end{aligned} \quad (34)$$

According to Assumption 1 and Young's inequality, it is obtained that

$$\begin{aligned} s_{1,j}^\top \Upsilon_{1,j} \frac{d_j}{m_j} & \leq \frac{\bar{d}_j^2}{2m_j^2\epsilon_j} s_{1,j}^\top \Upsilon_{1,j}^\top \Upsilon_{1,j}s_{1,j} + \frac{\epsilon_j}{2} \\ s_{3,j}^\top \tau_{d,j} & \leq \frac{\bar{\tau}_{d,j}^2}{2\epsilon_j} s_{3,j}^\top s_{3,j} + \frac{\epsilon_j}{2} \end{aligned} \quad (35)$$

where ϵ_j is a positive constant.

From (7), the unknown nonlinear functions $f_{n,j}$, $n = 1, 2, 3$ can be approximated by the RBFNNs as follows:

$$f_{n,j} = W_{n,j}^\top \Phi_{n,j} + \varepsilon_{n,j}. \quad (36)$$

Substituting (15), (27), (35), and (36) into (34) yields

$$\begin{aligned} \dot{V} \leq & -\bar{k}_{1,j}s_{1,j}^\top s_{1,j} - k_{2,j}s_{2,j}^\top s_{2,j} - k_{3,j}s_{3,j}^\top s_{3,j} \\ & + s_{1,j}^\top \varepsilon_{1,j} + s_{2,j}^\top \varepsilon_{2,j} + s_{3,j}^\top \varepsilon_{3,j} \\ & + \sum_{n=1}^3 \sigma_{n,j} \text{tr}(\tilde{W}_{n,j}^\top \widehat{W}_{n,j}) + \epsilon_j. \end{aligned} \quad (37)$$

According to Assumption 1 and Young's inequality, (37) can be expressed as follows:

$$\begin{aligned} \dot{V} \leq & -\left(\bar{k}_{1,j} - \frac{1}{2}\right) s_{1,j}^\top s_{1,j} - \left(k_{2,j} - \frac{1}{2}\right) s_{2,j}^\top s_{2,j} \\ & - \left(k_{3,j} - \frac{1}{2}\right) s_{3,j}^\top s_{3,j} - \sum_{n=1}^3 \frac{\sigma_{n,j}}{2} \|\tilde{W}_{n,j}\|_F^2 \\ & + \frac{1}{2} \sum_{n=1}^3 (\bar{\varepsilon}_{n,j}^2 + \sigma_{n,j} \overline{W}_{n,j}^2) + \epsilon_j. \end{aligned} \quad (38)$$

Choosing $\bar{k}_{1,j} = 0.5 + k_{1,j}^*$, $k_{2,j} = 0.5 + k_{2,j}^*$, and $k_{3,j} = 0.5 + k_{3,j}^*$ with positive constants $k_{n,j}^*$ for $n = 1, 2, 3$ yields

$$\dot{V} \leq -2c_0V + c_1, \quad (39)$$

where $c_0 = \min\{k_{1,j}^*, k_{2,j}^*, k_{3,j}^*, \lambda_{j_1}^{-1}, \lambda_{\sigma_{1,j}\Gamma_{1,j}}, \lambda_{\sigma_{2,j}\Gamma_{2,j}}, \lambda_{\sigma_{3,j}\Gamma_{3,j}}\}$ and $c_1 = \sum_{n=1}^3 (\bar{\varepsilon}_{n,j}^2 + \sigma_{n,j} \overline{W}_{n,j}^2)/2 + \epsilon_j$. $\lambda_{(\cdot)}$ denotes

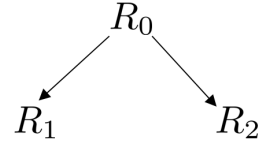


FIGURE 2. Connection between quadrotors.

the minimum eigenvalue of the matrix (\cdot) . Integrating both sides of (39) yields

$$V(t) \leq \left(V(0) - \frac{c_1}{2c_0} \right) \exp(-2c_0t) + \frac{c_1}{2c_0} \quad (40)$$

Therefore, $V(t) \leq \max\{V(0), c_1/(2c_0)\}$ is ensured. Since $V(0)$ and $c_1/(2c_0)$ are bounded, $s_{n,j}$ and $\tilde{W}_{n,j}$ for $n = 1, 2, 3$ are in \mathcal{L}_∞ . The optimal weights $W_{n,j}$ and Gaussian functions $\Phi_{n,j}$ of RBFNNs for $n = 1, 2, 3$ are bounded by Property 1 and the definitions of $\Phi_{n,j}$, respectively. Then, from (14), the compensating signals $\xi_{n,j}$ for $n = 1, 2, 3$ are bounded. Because $s_{1,j}$ and $\xi_{1,j}$ are bounded, it holds that $e_{11,j} \in \mathcal{L}_\infty$. Therefore, it is ensured that $r_{a,j} < l_{ij}(t) < r_{c,j}$ for $t \geq 0$.

From Property 1, (13), (14), and (40), the following inequalities are obtained:

$$\begin{aligned} \|\widehat{W}_{1,j}\|_F & \leq \overline{W}_{1,j} + \sqrt{\frac{c_1}{c_0\lambda_{\Gamma_{1,j}}^{-1}}} \\ \|\xi_{1,j}\| & \leq \frac{\|\widehat{W}_{1,j}\|_F \|\Phi_{1,j}\|}{\lambda_{k_{1,j}}} \leq \frac{\sqrt{N_j}}{\lambda_{k_{1,j}}} \left(\overline{W}_{1,j} + \sqrt{\frac{c_1}{c_0\lambda_{\Gamma_{1,j}}^{-1}}} \right) \\ \|e_{1,j}\| & \leq \frac{1}{\lambda_{\Lambda_{1,j}}} \left(\|\xi_{1,j}\| + \sqrt{\frac{c_1}{c_0}} \right) \leq \mu_1 \end{aligned}$$

$$|l_{d,ij} - l_{ij}| \leq \mu_0$$

$$|\alpha_{d,ij} - \alpha_{ij}| \leq \mu_1, \quad |\beta_{d,ij} - \beta_{ij}| \leq \mu_1$$

where

$$\begin{aligned} \mu_0 & = \min \left\{ \left| \frac{(r_{c,j} - l_{d,ij})(e^{-\mu_1} - 1)}{1 + h_{ij}e^{-\mu_1}} \right|, \right. \\ & \quad \left. \left| \frac{(r_{c,j} - l_{d,ij})(e^{\mu_1} - 1)}{1 + h_{ij}e^{\mu_1}} \right| \right\} \\ \mu_1 & = \frac{1}{\lambda_{\Lambda_{1,j}}} \left(\frac{\sqrt{N_j}}{\lambda_{k_{1,j}}} \left(\overline{W}_{1,j} + \sqrt{\frac{c_1}{c_0\lambda_{\Gamma_{1,j}}^{-1}}} \right) + \sqrt{\frac{c_1}{c_0}} \right). \end{aligned}$$

Here, $\lambda_{\Gamma_{1,j}^{-1}}$, $\lambda_{k_{1,j}}$, and $\lambda_{\Lambda_{1,j}}$ denote the minimum eigenvalues of $\Gamma_{1,j}^{-1}$, $k_{1,j}$, and $\Lambda_{1,j}$, respectively. Therefore, design parameters exist to achieve the control objectives. In addition, μ_0 and μ_1 can be made arbitrarily small by increasing $\lambda_{k_{1,j}}$, $\lambda_{\Lambda_{1,j}}$, and c_0 , and thus the desired safety formation of multiple quadrotors is achieved. This completes the proof of Theorem 1. ■

Remark 7: In this paper, the inertia matrix J_j of the quadrotor is assumed to be unknown. The effects of model uncertainties that may be present in the inertia matrix J_j can be considered in the unknown nonlinear function $f_{3,j}$ (see (33)).

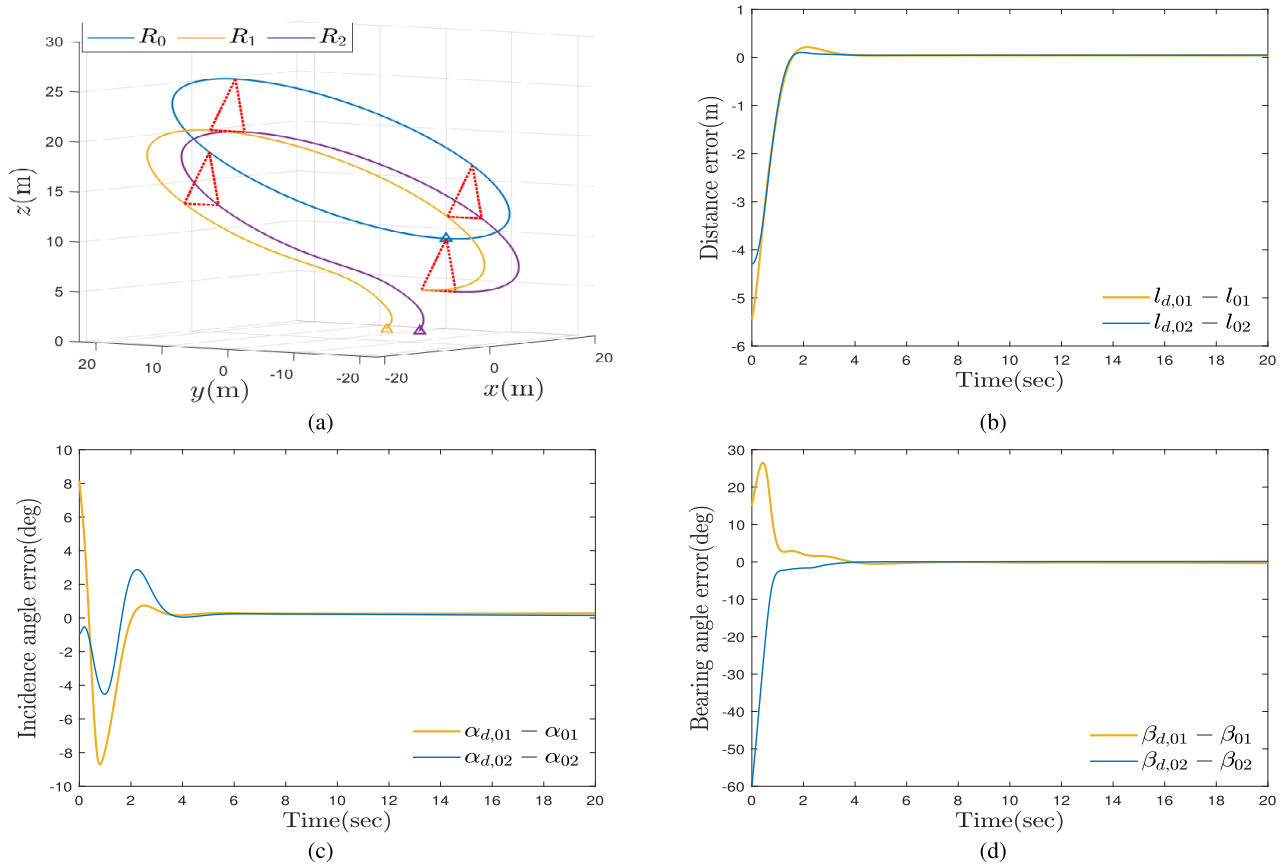


FIGURE 3. Simulation results for Section IV-A (a) trajectory (b) distance error (c) incidence angle error (d) bearing angle error.

TABLE 1. RMS values at steady-state response under various design parameters.

Design parameters	R_1	R_2
$k_{1,j} = 3, k_{2,j} = 3, k_{3,j} = 2$	0.0431	0.0472
$k_{1,j} = 5, k_{2,j} = 5, k_{3,j} = 5$	0.026	0.0287
$k_{1,j} = 7, k_{2,j} = 7, k_{3,j} = 7$	0.0186	0.0206

The function approximation technique using the RBFNN is employed to compensate for the unknown nonlinear function $f_{3,j}$. Then, we use the output of the RBFNN to design the control torque τ_j , as shown in (25). This implies that the proposed controller can be implemented even when the inertia matrix is fully unknown, ensuring the robustness of the proposed method in the presence of uncertainty in the inertia matrix. However, if the inertia matrix is not diagonal, and we cannot guarantee the positive-definiteness of the inertia matrix, then the controller should be redesigned using adaptive control or robust control techniques to account for the uncertain inertia matrix. While this problem is not the primary focus of our study, it is a topic worth investigating in future research.

Remark 8: Compared with the existing work using unified formation errors for nonholonomic mobile robots [28], the nonlinear quadrotors (i.e., (1) and (2)) considered in this study have the difficulty in designing the formation controller because of highly nonlinear couplings and fewer control

TABLE 2. RMS values for formation errors and control inputs.

	proposed method	RB-SMC method
formation errors of R_1	0.68	0.68
formation errors of R_2	0.71	0.71
control inputs of R_1	1.75	19.33
control inputs of R_2	2.02	15.35

inputs, as stated in Remark 2. In other words, the previous approach [28] for nonholonomic mobile robots cannot be directly extended to the quadrotor model. To address this problem, we propose the state-transformation-based design strategy using the unified formation error to guarantee formation tracking and collision avoidance of uncertain multiple quadrotors.

IV. SIMULATION RESULTS

In this section, two cases are simulated to verify the effectiveness of the proposed method using MATLAB on a computer with an AMD Ryzen 5 2600 processor operating at 3.4GHz. Three quadrotors with one leader ($i = 0$) and two followers ($j = 1, 2$) are considered, as shown in Fig. 2. The model parameters of the followers are taken from [31] as follows: $m_j = 4.34$ kg, $J_{x,j} = 0.082$ kg·m², $J_{y,j} = 0.0845$ kg·m², $J_{z,j} = 0.1377$ kg·m², and $g = 9.8$ m/s². The disturbance vectors are considered as $d_j = [\sin(t), \sin(t), \cos(t)]^T$ and

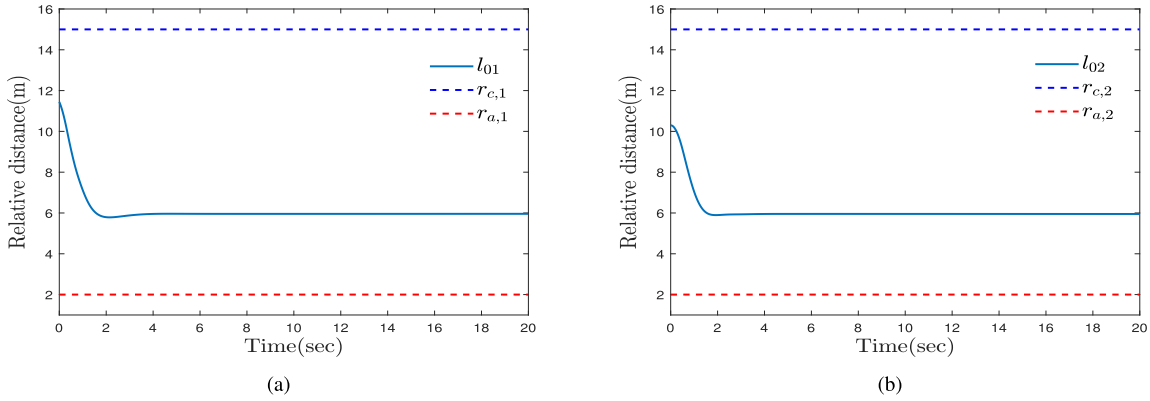


FIGURE 4. Relative distance for Section IV-A (a) follower 1 (b) follower 2.

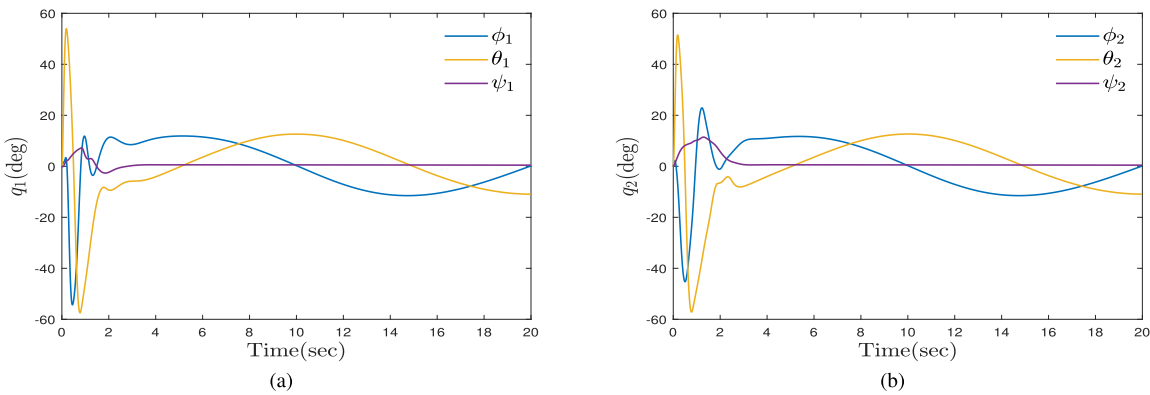


FIGURE 5. Euler angles for Section IV-A (a) follower 1 (b) follower 2.

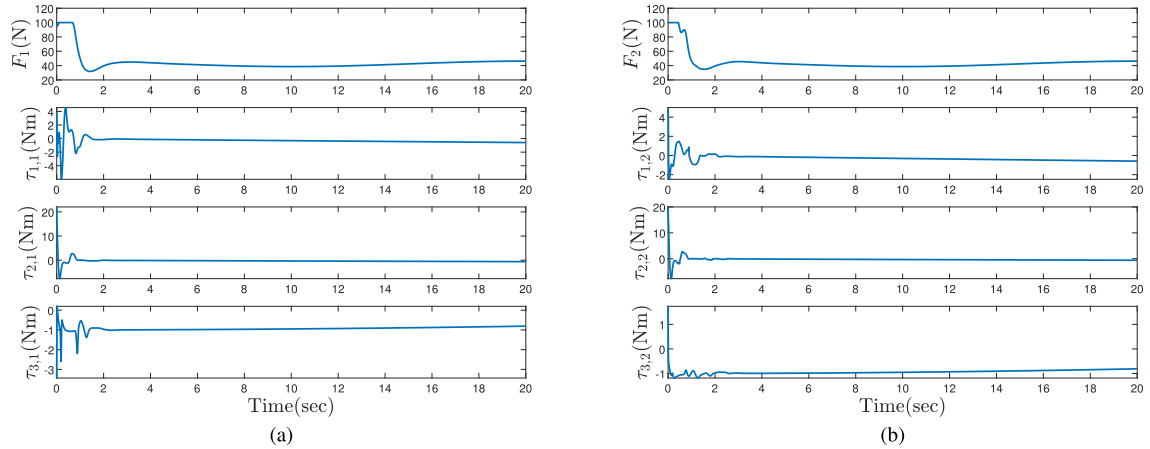


FIGURE 6. Control inputs for Section IV-A (a) follower 1 (b) follower 2.

$\tau_{d,j} = [\sin(\pi t), \sin(\pi t), \cos(\pi t)]^T$. For the RBFNNs, the number of hidden layer nodes and width of the Gaussian function are chosen as $N_j = 3$ and $\zeta_{n,h,j} = 1$, respectively.

A. VERIFICATION OF THEORETICAL RESULTS

The trajectory of the leader is generated by $p_0 = [20 \cos(\pi t/10) \text{ m}, 20 \sin(\pi t/10) \text{ m}, 18 - 9 \cos(\pi t/10) \text{ m}]^T$

and $\psi_0 = 0$ rad. The initial position vectors of followers are selected as $p_1(0) = [15 \text{ m}, 5 \text{ m}, 0 \text{ m}]^T$ and $p_2(0) = [15 \text{ m}, 0 \text{ m}, 0 \text{ m}]^T$. The desired distance and angles of incidence and bearing are set as $l_{d,01} = l_{d,02} = 6 \text{ m}$, $\psi_{d,1} = 0 \text{ rad}$, $\psi_{d,2} = 0 \text{ rad}$, $\alpha_{d,01} = \pi/3 \text{ rad}$, $\alpha_{d,02} = -\pi/3 \text{ rad}$, $\beta_{d,01} = \pi/3 \text{ rad}$, and $\beta_{d,02} = -\pi/3 \text{ rad}$. The measurement and avoidance ranges are set to $r_{c,j} = 15 \text{ m}$ and $r_{a,j} = 2 \text{ m}$.

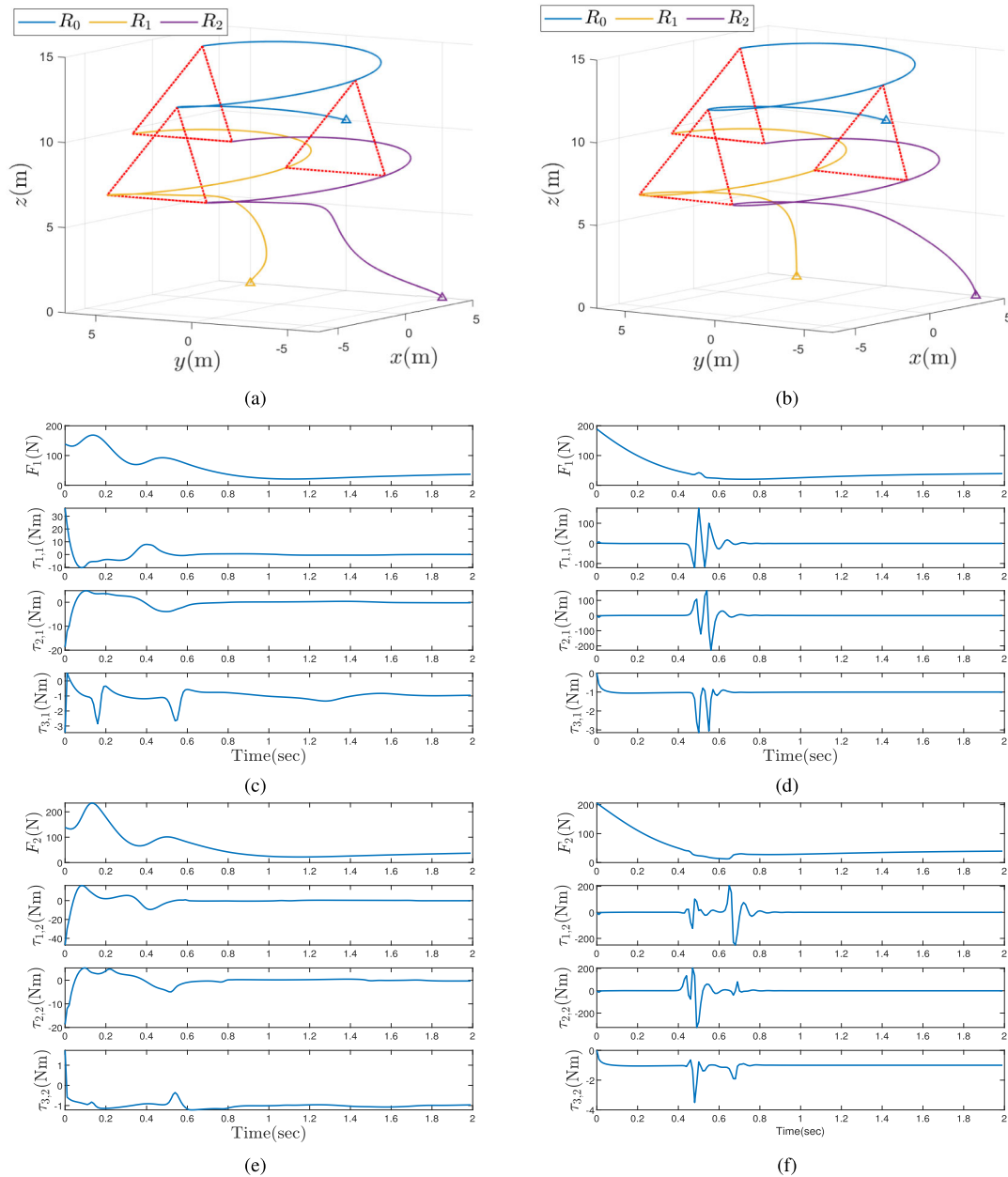


FIGURE 7. Simulation comparison results for Section IV-B (a) trajectory of the proposed method (b) trajectory of the RB-SMC method (c) control inputs of the follower 1 using proposed method (d) control inputs of the follower 1 using RB-SMC method (e) control inputs of the follower 2 using proposed method (f) control inputs of the follower 2 using RB-SMC method.

The lower and upper bounds of F_j are $F_{m,j} = 20$ N and $F_{M,j} = 100$ N. The design parameters are chosen as $\bar{k}_{1,j} = k_{2,j} = 3$, $k_{3,j} = 2$, $\gamma_{n,j} = 100$, $\Lambda_{1,j} = \text{diag}[1.5, 1.5, 1.5]$, $\Gamma_{n,j} = \text{diag}[3, 3, 3]$, and $\sigma_{n,j} = 0.1$ where $n = 1, 2, 3$.

The simulation results are shown in Figs. 3–6. Fig. 3 shows the trajectories of multiple quadrotors and the formation tracking errors. The distance, incidence angle, and bearing angle errors are bounded and converge to nearly zero. Fig. 4 depicts the relative distances between the leader and followers. The relative distances for all followers are within the range $r_{a,j} < l_{ij} < r_{c,j}$. Therefore, the theoretical results of

Theorem 1 are verified from Figs. 3 and 4. The Euler angles of the followers are displayed in Fig. 5. The Euler angles vary by close to $\pm 60^\circ$. Thus, the proposed method is effective in a wide operating range, unlike the linear control methods. Fig. 6 shows the control inputs of the followers. The thrust forces are saturated within $t = 1$ s due to initial errors, and the torques are not large. To measure the computation time, the tic and toc functions of MATLAB are used. The average time required for the computation per step of each quadrotor is $t = 0.0013$ s. To analyze the change in formation errors based on design parameters, a simulation is conducted using several

design parameters. The root-mean-square (RMS) values of the formation error vector $e_{1,j}$ at the steady-state response are calculated and presented in Table 1, where the formation errors for $t \geq 8$ s are defined for the steady-state response. The results indicate that the increase in the design parameters decreases formation errors, as stated in Theorem 1. Overall, the proposed method is effective in achieving the desired safety formation despite the saturation of thrust forces.

B. COMPARISON RESULTS

Comparative analyses are performed to demonstrate the superiority of the proposed method over the robust backstepping sliding mode control (RB-SMC) method [32], which uses the hierarchical strategy. In the RB-SMC method, the virtual references for formation tracking are generated using $x_{r,j} = l_{d,ij} \cos \alpha_{d,ij} \cos(\psi_i - \beta_{d,ij})$, $y_{r,j} = l_{d,ij} \cos \alpha_{d,ij} \sin(\psi_i - \beta_{d,ij})$, and $z_{r,j} = l_{d,ij} \sin \alpha_{d,ij}$ because only a single quadrotor is considered. The trajectory of the leader is given by $p_0 = [5 \cos(\pi t/10), 4 \sin(\pi t/10), 10 + 5 \sin(\pi t/60)]^T$ and $\psi_0 = 0$. The initial position vectors of followers are selected as $p_1(0) = [5, 5, 0]^T$ and $p_2(0) = [5, -5, 0]^T$. The parameters related to the desired safety formation are set to be identical to those presented in Section IV-A. To show the effectiveness of the control inputs, the design parameters are set such that both methods have the same errors. The RMS values are used to compare the formation errors and control inputs.

Fig. 7 displays the comparison results, where the transient responses of control inputs are compared in Figs. 7(c)-(f). Both methods achieve the desired formation, but the RB-SMC method requires greater torque inputs than the proposed method. This phenomenon occurs because the hierarchical-strategy-based control method requires higher gains for attitude controllers than the proposed method. Table 2 provides the detailed results for the formation errors and control inputs, further supporting the conclusion that the proposed method is more energy-efficient than the control methods based on the hierarchical strategy.

V. CONCLUSION

In this study, a unified state-transformation-based design strategy was presented for adaptive leader-follower safety formation control of range-constrained uncertain quadrotors with unknown disturbances and thrust saturation. A novel state-transformation-based control method was developed to solve the underactuation and nonlinear input coupling problems of quadrotors and a recursive design was obtained using the Euler angles directly without dividing the outer and inner loop subsystems. The proposed approach ensured a formation tracking performance similar to that of the hierarchical design strategy with lower torque inputs, which helps increase the operation time of quadrotors. Additionally, the unified error-based design ensured safe formation tracking without the input coupling problem of existing APF-based designs, and allowed a wide operating range of the Euler angles. The closed-loop stability of the proposed control system was analyzed in the Lyapunov sense and the comparative

simulation results were provided. In this paper, the yaw angle of the leader was only transmitted to followers using a wireless communication device. Thus, further extensions to the leader-follower safety formation control problem in the presence of communication delay can be investigated for future research.

REFERENCES

- [1] J. Tang, G. Liu, and Q. Pan, "A review on representative swarm intelligence algorithms for solving optimization problems: Applications and trends," *IEEE/CAA J. Autom. Sinica*, vol. 8, no. 10, pp. 1627–1643, Oct. 2021.
- [2] J. Tang, X. Chen, X. Zhu, and F. Zhu, "Dynamic reallocation model of multiple unmanned aerial vehicle tasks in emergent adjustment scenarios," *IEEE Trans. Aerosp. Electron. Syst.*, vol. 59, no. 2, pp. 1139–1155, Apr. 2023, doi: 10.1109/TAES.2022.3195478.
- [3] Y. Q. Chen and Z. Wang, "Formation control: A review and a new consideration," in *Proc. IEEE/RSJ Int. Conf. Intell. Robots Syst.*, Edmonton, AB, Canada, Aug. 2005, pp. 3181–3186.
- [4] A. Mondal, C. Bhowmick, L. Behera, and M. Jamshidi, "Trajectory tracking by multiple agents in formation with collision avoidance and connectivity assurance," *IEEE Syst. J.*, vol. 12, no. 3, pp. 2449–2460, Sep. 2018.
- [5] Z. Zhao, J. Wang, Y. Chen, and S. Ju, "Iterative learning-based formation control for multiple quadrotor unmanned aerial vehicles," *Int. J. Adv. Robot. Syst.*, vol. 17, no. 2, pp. 1–12, 2020.
- [6] F. Rinaldi, S. Chiesa, and F. Quagliotti, "Linear quadratic control for quadrotors UAVs dynamics and formation flight," *J. Intell. Robot. Syst.*, vol. 70, nos. 1–4, pp. 203–220, 2013.
- [7] Q. Yuan, J. Zhan, and X. Li, "Outdoor flocking of quadcopter drones with decentralized model predictive control," *ISA Trans.*, vol. 71, pp. 84–92, Nov. 2017.
- [8] A. Mahmood and Y. Kim, "Leader-following formation control of quadcopters with heading synchronization," *Aerosp. Sci. Technol.*, vol. 47, no. 1, pp. 68–74, Dec. 2015.
- [9] A. Tahir, J. M. Böling, M.-H. Haghbayan, and J. Plosila, "Comparison of linear and nonlinear methods for distributed control of a hierarchical formation of UAVs," *IEEE Access*, vol. 8, pp. 95667–95680, 2020.
- [10] X. Dong, Y. Zhou, Z. Ren, and Y. Zhong, "Time-varying formation tracking for second-order multi-agent systems subjected to switching topologies with application to quadrotor formation flying," *IEEE Trans. Ind. Electron.*, vol. 64, no. 6, pp. 5014–5024, Jun. 2017.
- [11] W. Jasim and D. Gu, "Robust team formation control for quadrotors," *IEEE Trans. Control Syst. Technol.*, vol. 26, no. 4, pp. 1516–1523, Jul. 2018.
- [12] J. Wang, X. Ma, H. Li, and B. Tian, "Self-triggered sliding mode control for distributed formation of multiple quadrotors," *J. Franklin Inst.*, vol. 357, no. 17, pp. 12223–12240, Nov. 2020.
- [13] J. Wang, C. Bi, D. Wang, Q. Kuang, and C. Wang, "Finite-time distributed event-triggered formation control for quadrotor UAVs with experimentation," *ISA Trans.*, vol. 126, pp. 585–596, Jul. 2022.
- [14] Y. Ouyang, L. Xue, L. Dong, and C. Sun, "Neural network-based finite-time distributed formation-containment control of two-layer quadrotor UAVs," *IEEE Trans. Syst., Man, Cybern. Syst.*, vol. 52, no. 8, pp. 4836–4848, Aug. 2022.
- [15] Y. Yu, J. Guo, C. K. Ahn, and Z. Xiang, "Neural adaptive distributed formation control of nonlinear multi-UAVs with unmodeled dynamics," *IEEE Trans. Neural Netw. Learn. Syst.*, early access, Mar. 16, 2022, doi: 10.1109/TNNLS.2022.3157079.
- [16] H. Liu, T. Ma, F. L. Lewis, and Y. Wan, "Robust formation control for multiple quadrotors with nonlinearities and disturbances," *IEEE Trans. Cybern.*, vol. 50, no. 4, pp. 1362–1371, Apr. 2020.
- [17] W. Zhao, H. Liu, and F. L. Lewis, "Robust formation control for cooperative underactuated quadrotors via reinforcement learning," *IEEE Trans. Neural Netw. Learn. Syst.*, vol. 32, no. 10, pp. 4577–4587, Oct. 2021.
- [18] G. Wang, Y. Yang, N. Zhao, Y. Ji, Y. Shen, H. Xu, and P. Li, "Distributed consensus control of multiple UAVs in a constrained environment," in *Proc. IEEE Int. Conf. Robot. Autom. (ICRA)*, Paris, France, May 2020, pp. 3234–3240.
- [19] F. Liao, R. Teo, J. L. Wang, X. Dong, F. Lin, and K. Peng, "Distributed formation and reconfiguration control of VTOL UAVs," *IEEE Trans. Control Syst. Technol.*, vol. 25, no. 1, pp. 270–277, Jan. 2017.

- [20] Y. Huang, W. Liu, B. Li, Y. Yang, and B. Xiao, "Finite-time formation tracking control with collision avoidance for quadrotor UAVs," *J. Franklin Inst.*, vol. 357, no. 7, pp. 4034–4058, May 2020.
- [21] W. Shang, G. Jing, D. Zhang, T. Chen, and Q. Liang, "Adaptive fixed time nonsingular terminal sliding-mode control for quadrotor formation with obstacle and inter-quadrotor avoidance," *IEEE Access*, vol. 9, pp. 60640–60657, 2021.
- [22] Y. Yang, L. Liao, H. Yang, and S. Li, "An optimal control strategy for multi-UAVs target tracking and cooperative competition," *IEEE/CAA J. Autom. Sinica*, vol. 8, no. 12, pp. 1931–1947, Dec. 2021.
- [23] Z. Pan, C. Zhang, Y. Xia, H. Xiong, and X. Shao, "An improved artificial potential field method for path planning and formation control of the multi-UAV systems," *IEEE Trans. Circuits Syst. II, Exp. Briefs*, vol. 69, no. 3, pp. 1129–1133, Mar. 2022.
- [24] O. Souissi, R. Benatitallah, D. Duvivier, A. Artiba, N. Belanger, and P. Feyzeau, "Path planning: A 2013 survey," in *Proc. Int. Conf. Ind. Eng. Syst. Manag.*, Agdal, Morocco, 2013, pp. 1–8.
- [25] S. Bouabdallah and R. Siegwart, "Backstepping and sliding-mode techniques applied to an indoor micro quadrotor," in *Proc. IEEE Int. Conf. Robot. Autom.*, Barcelona, Spain, Apr. 2005, pp. 2247–2252.
- [26] J. Park and I. W. Sandberg, "Universal approximation using radial-basis-function networks," *Neural Comput.*, vol. 3, no. 2, pp. 246–257, Jun. 1991.
- [27] S. S. Ge and C. Wang, "Adaptive neural control of uncertain MIMO nonlinear systems," *IEEE Trans. Neural Netw.*, vol. 15, no. 3, pp. 674–692, May 2004.
- [28] S. J. Yoo and B. S. Park, "Connectivity preservation and collision avoidance in networked nonholonomic multi-robot formation systems: Unified error transformation strategy," *Automatica*, vol. 103, pp. 274–281, May 2019.
- [29] W. Dong, J. A. Farrell, M. M. Polycarpou, V. Djapic, and M. Sharma, "Command filtered adaptive backstepping," *IEEE Trans. Control Syst. Technol.*, vol. 20, no. 3, pp. 566–580, May 2012.
- [30] G. Wang, W. Yang, N. Zhao, Y. Shen, and C. Wang, "An approximation-free simple controller for uncertain quadrotor systems in the presence of thrust saturation," *Mechatronics*, vol. 72, Dec. 2020, Art. no. 102450.
- [31] P. Pounds, R. Mahony, and P. Corke, "Modelling and control of a large quadrotor robot," *Control Eng. Pract.*, vol. 18, no. 7, pp. 691–699, Jul. 2010.
- [32] F. Chen, R. Jiang, K. Jiang, and B. Tao, "Robust backstepping sliding mode control and observer-based fault estimation for a quadrotor UAV," *IEEE Trans. Ind. Electron.*, vol. 63, no. 8, pp. 5044–5056, Aug. 2016.



BONG SEOK PARK received the B.S., M.S., and Ph.D. degrees in electrical and electronic engineering from Yonsei University, in 2005, 2008, and 2011, respectively. Since 2015, he has been with the Division of Electrical, Electronic, and Control Engineering, Kongju National University. His research interests include nonlinear control, formation control, and the control of robots.



SUNG JIN YOO (Member, IEEE) received the B.S., M.S., and Ph.D. degrees in electrical and electronic engineering from Yonsei University, Seoul, South Korea, in 2003, 2005, and 2009, respectively. He was a Postdoctoral Researcher with the Department of Mechanical Science and Engineering, University of Illinois at Urbana-Champaign, Illinois, from 2009 to 2010. Since 2011, he has been with the School of Electrical and Electronics Engineering, Chung-Ang University, Seoul, where he is currently a Professor. His research interests include nonlinear adaptive control, decentralized control, distributed control, fault-tolerant control, and neural networks theories and their applications to robotic, flight, nonlinear time-delay systems, large-scale systems, and multi-agent systems. He is an Associate Editor of *IEEE TRANSACTIONS ON CYBERNETICS* and *International Journal of Control, Automation, and Systems*.

• • •